Studies of Framework Iron in Zeolites by Pulsed ENDOR at 95 GHz

D. Goldfarb,*,† K. G. Strohmaier,‡ D. E. W. Vaughan,‡ H. Thomann,‡,§ O. G. Poluektov,⊥ and J. Schmidt⊥

Contribution from the Department of Chemical Physics, Weizmann Institute of Science, 76100 Rehovot, Israel, Exxon Research and Engineering Co., Route 22 East, Annandale, New Jersey 08801, and Huygens Laboratory, Leiden University, P.O. Box 9504, 2300 RA Leiden, The Netherlands

Received November 21, 1995[⊗]

Abstract: High frequency (95 GHz, W-band) pulsed ENDOR measurements were carried out on the ^{57}Fe-containing zeolites: Fe-sodalite (FeSOD), Fe-L (FeLTL), Fe-mazzite (FeMAZ), and Fe-ZSM5 (FeMFI), where ^{57}Fe(III) was introduced during synthesis. The echo-detected EPR spectra of all zeolites investigated, recorded at 1.8 K, show mainly the $|-^5/_2\rangle$ to $|-^3/_2\rangle$ EPR transition. Accordingly, the ENDOR spectra exhibit only two ^{57}Fe ENDOR transitions at 67.8−68.8 and 39.0−39.6 MHz, corresponding to $M_S = -^5/_2$ and $-^3/_2$, respectively. From these frequencies isotropic hyperfine couplings of −29.0, −29.3, −29.5, and −29.6 MHz were derived for ^{57}FeSOD, ^{57}FeL, ^{57}FeMAZ, and ^{57}FeMFI, respectively. On the basis of an earlier assignment of the $g = 2$ signal in FeSOD to Fe(III) in tetrahedral framework sites it is concluded that hyperfine couplings in the range −29.0 to −29.6 MHz are characteristic of ^{57}Fe(III) in zeolite frameworks. In contrast to the X-band ^{57}Fe ENDOR signals, the W-band signals are free from second- and third-order contributions of the hyperfine and zero-field splitting (ZFS) interactions and are thus significantly simpler to assign and interpret. The ZFS contributions caused excessive inhomogeneous broadening of the X-band ENDOR spectra of ^{57}FeL, ^{57}FeMAz, and ^{57}FeMFI and the detection of the ENDOR spectra was practically impossible: All zeolites studied exhibited ENDOR signals from ^{27}Al and ^{57}FeSOD showed also clear ^{23}Na ENDOR signals. The hyperfine interaction of the ^{23}Na was significantly larger than that of the ^{27}Al, confirming the assignment of the Fe(III) to framework sites, substituting for Al. Moreover, the value obtained for the ^{23}Na anisotropic hyperfine component, 0.53 MHz, corresponding to a distance of 3.4 Å, is in good a agreement with the known structure of sodalite where the distance between a framework atom and the Na^+ cations in the center of the six rings is 3.35 Å. This work demonstrates the power and potential of high-field ENDOR in terms of resolution, signal assignment, and spectral analysis.

Introduction

The prospect of transition metal incorporation into the framework of aluminosilicate and aluminophosphate molecular sieves has been drawing a continuous interest among researchers due to the potential new catalytic properties of the modified materials. These for instance can be expressed in oxidation/reduction activity and/or in the modification of the acidity, depending on the nature and loading of the transition metal and on the molecular sieve structure. One of the most extensively studied transition metals in the context of framework substitution has been iron. In many natural and synthetic zeolites it is found as an impurity,[1−3] and there have been numerous reports on its successful incorporation into the frameworks of zeolites and aluminophosphate molecular sieves.[3−14] In these materials the iron usually does not occupy exclusively tetrahedral (T) framework sites. It can also exist as extra-framework cations and/or as an interstitial phase of small particles located either within the zeolite pores or on its external surface.[1−3,9,10] The techniques commonly used to characterize iron sites in molecular sieves and oxide catalysts include Mössbauer, UV−vis, IR, and EPR spectroscopies[3,15] and extended X-ray absorption fine structure (EXAFS).[9−11] Unambiguous assignment of the iron sites usually requires a combination of several methods.

We have recently investigated the feasibility of using pulsed electron-nuclear double resonance (ENDOR) spectroscopy of ^{57}Fe ($I = ^1/_2$) combined with EPR spectroscopy as an additional tool for the characterization of Fe(III) sites in zeolites.[16] The ENDOR spectrum provides the ^{57}Fe hyperfine interaction which in turn gives information on local geometry and bonding

† Weizmann Institute of Science.
‡ Exxon Research and Engineering Co.
§ Also Department of Chemistry, State University of New York, Stony Brook.
⊥ Leiden Universlty.
⊗ Abstract published in *Advance ACS Abstracts,* April 15, 1996.

(1) McNicol, B. D.; Pott, G. T. *J. Catal.* **1972**, *25*, 223.
(2) Derouane, G. T.; Mestdagh, M.; Vielvoye, I. *J. Catal.* **1974**, *33*,169.
(3) Ratnasami O.; Kumar, R. *Catal. Today* **1991**, *9*, 328.
(4) Zi, G.; Dake, T.; Ruiming, Z. *Zeolites* **1988**, *8*, 453.
(5) Kotasthane, A. N.; Shiralkar, V. P.; Hegde, S. G.; Kulkarni, S. B. *Zeolites* **1986**, *6*, 253.
(6) Inui, T.; Nagata, H.; Takeguchi, T.; Iwamato, S.; Matsuda, H.; Inoue, M. *J. Catal.* **1993**, *139*, 482.
(7) Lin, D. H.; Coudurier, G.; Vedrine, J. In *Zeolites: Facts, Figures, Future*; Jacobs, P. A., van Santen, R. A., Eds.; Elsevier Science Publishers: B. V. Amsterdam, The Netherlands, **1989**; p 1431.
(8) Patarin, J.; Tuilier, M.; Durr, J.; Kessler, H. *Zeolites* **1992**, *12*, 70.
(9) Pickering, I. J.; Vaughan, D. E. W.; Strohmaier, K. G.; George, G. N.; Via, G. H. In *Proceedings of the 9th International Zeolite Conference*; von Ballmoos, R., Treacy, M. M. J., Higgins, J. B., Eds.; Butterworths/Heinemann: Stoneham, MA, **1993**; p 197.
(10) Vaughan, D. E. W.; Strohmaier, K. G.; Pickering, I. J.; George, G. N. *Solid State Ionics* **1992**, *53−56*, 1282.
(11) Axon, S. A.; Fox, K. K.; Carr, S. W.; Klinowski, J. *Chem. Phys. Lett.* **1992**, *189*, 1.
(12) Flanigen, E. M.; Lok, B. M. T. K.; Patton, R. L.; Wilson, S. T. *Stud. Surf. Sci. Catal.* **1986**, *28*, 109.
(13) Joshi, P. N.; Awate, S. V.; Shiralkar, V. P. *J. Phys. Chem.* **1993**, *97*, 9749.
(14) Lázár, K.; Borbely, G.; Beyer, H. *Zeolites* **1991**, *11*, 214.
(15) Goldfarb, D.; Bernardo, M.; Strohmaier, K. G.; Vaughan, D. E. W.; Thomann, H. *J. Am. Chem. Soc.* **1994**, *116*, 6344.

S0002-7863(95)03903-5 CCC: $12.00

Table 1. The Composition of the Zeolites Investigated, Given in Relative Atom %

sample	zeolite	T sites	Fe	Al	Si	Na	K	$\frac{Fe}{Fe+Al+Si}$ [a]	ref[b]
^{57}FeSOD	sodalite	1	0.001	0.999	0.96	1.32		0.05	10
^{57}FeLTL	Linde L	2	0.002	0.998	2.71		1.01	0.07	9
^{57}FeMAZ	mazzite	2	0.003	0.997	2.92	0.78		0.07	23
^{57}FeMFI	ZSM5	12	0.0018	0.982	28.2	0.65		0.06	24

[a] Molar ratio of Fe expressed as a molar percent. [b] Synthesized according to these references.

characteristics such as the degree of covalency.[17] The hyperfine interaction of ^{57}Fe can also be determined by Mössbauer spectroscopy, but pulsed ENDOR provides additional resolution obtained from the EPR spectrum. Furthermore, the versatility of the pulsed ENDOR experiments offers a larger scope for resolving and assigning signals.[18]

The hyperfine interaction of ^{57}Fe(III) (d^5, $S = {}^5/_2$, $I = {}^1/_2$) is predominately isotropic[17] and the ENDOR frequencies, given to second order, are[19]

$$\nu(M_S)_{M_I \leftrightarrow M_{I+1}} = \left| -\nu_L + M_S a_{iso} - \frac{a_{iso}^2 M_S}{\nu_e}\left(M_I + M_S + \frac{1}{2}\right)\right| \quad (1)$$

where ν_e and ν_L are the electronic and nuclear Larmor frequencies, respectively, and a_{iso} is the isotropic hyperfine constant. The first-order ^{57}Fe(III) ENDOR spectrum consists of three doublets, centered at ${}^1/_2 a_{iso}$, ${}^3/_2 a_{iso}$ and ${}^5/_2 a_{iso}$, and each doublet is split by $2\nu_L$. The higher order perturbation terms cause deviations of the splitting of the doublets from $2\nu_L$ (see eq 1) and shift the center of the doublets.[20]

X-band ($\approx$ 9.2 GHz) pulsed ENDOR spectra of ^{57}Fe in sodalite (^{57}FeSOD), recorded at $g = 2$ ($H_o = 3317$ G), showed three doublets centered at 14.86, 43.87, and 72.09 MHz with splittings of 1.2, 2.5, and 1.3 MHz, respectively.[16,21] These splittings deviate significantly from $2\nu_L$ which at this field is 0.96 MHz. These deviations cannot be accounted for just by taking into account the second-order effect of the hyperfine interaction. Moreover, ENDOR spectra recorded at different magnetic fields within the EPR powder pattern showed orientation dependence which was most significant for the peaks corresponding to the $M_S = \pm{}^1/_2$ and $\pm{}^3/_2$ manifolds.[21] Since the anisotropic hyperfine interaction of ^{57}Fe(III) is negligible,[17] this dependence has been attributed to contributions of the ZFS to the ENDOR frequencies and the orientation dependence could be reproduced in simulated spectra.[21] Line broadening attributed to the ZFS has also been observed in the ^{55}Mn(II) ENDOR lines of Concanavalin A.[20] While the ENDOR spectrum of ^{57}FeSOD was highly resolved,[16] the spectra of ^{57}Fe containing zeolite L (^{57}FeLTL), Mazzite (^{57}FeMAZ), and ZSM5 (^{57}FeMFI) exhibited very weak and broad signals that were barely detectable and highly orientation dependent.[22] The excessive broadening in these zeolites was attributed to the ZFS, which is significantly larger than in ^{57}FeSOD.[15]

In this work we present pulsed ENDOR measurements on ^{57}FeSOD, ^{57}FeLTL, ^{57}FeMAZ, and ^{57}FeMFI, performed at W-band (95 GHz), which demonstrate the power of high-field ENDOR spectroscopy. We show that at this frequency the third-order contribution of the ZFS to the ENDOR signals is negligible and that the ^{57}Fe hyperfine interaction is indeed isotropic. ENDOR spectra of ^{57}FeLTL and ^{57}FeMAZ, which could not be obtained at X-band frequencies, are readily observed at 95 GHz. The hyperfine coupling constants of the ^{57}Fe in all four zeolites are close, indicating that these values are typical for ^{57}Fe(III) in framework sites of zeolites. In the case of ^{57}FeSOD, ENDOR signals of ^{23}Na were observed as well. Analysis of the ^{23}Na powder patterns gave a value for the anisotropic hyperfine interaction which is in good agreement with a framework Fe(III) interacting with Na^+ ions in the center of the six-member ring, thus providing additional evidence for framework substitution.

Experimental Section

Synthesis. All zeolites were synthesized according to published procedures[9,10,23,24] using an enriched $^{57}FeCl_3$ solution prepared by dissolving $^{57}Fe_2O_3$ in excess 1 N HCl solution. The compositions of the zeolites studied are listed in Table 1.

ENDOR Measurements. The ENDOR spectra were recorded at 1.5 K on a pulsed spectrometer operating at 95 GHz described elsewhere.[25] Echo-detected (ED) EPR spectra were recorded using either the two-pulse sequence, $\pi/2-\tau-\pi-\tau-$echo, or the three-pulse sequence, $\pi/2-\tau-\pi/2-T-\pi/2-\tau-$echo, where the echo amplitude is measured as a function of the magnetic field and the time intervals τ and T are held constant. The ENDOR spectra were recorded using the Davies ENDOR ($\pi-T-\pi/2-\tau-\pi-\tau-$echo)[26] and Mims ENDOR ($\pi/2-\tau-\pi/2-T-\pi/2-\tau-$echo)[27] pulse sequences where a RF π pulse is introduced during the time interval T in both sequences. In both experiments the echo amplitude is recorded as a function of the RF frequency. Typical pulse durations for the microwave pulses were 0.050−0.15 and 0.1−0.3 μs for the $\pi/2$ and π pulses, respectively. The duration of the RF pulse (t_{RF}) was 50−200 μs and the repetition rate was 90 Hz. Depending on the S/N, 2−30 scans of 6 echoes per data point were accumulated for each spectrum.

Results

The ED-EPR spectra of ^{57}FeSOD, ^{57}FeLTL, ^{57}FeMAZ, and ^{57}FeMFI are shown in Figure 1. The spectra are dominated by the $|-{}^5/_2\rangle-|-{}^3/_2\rangle$ EPR transition since at 95 GHz and 1.5 K the only significantly populated energy level is that corresponding to $M_S = -{}^5/_2$ (the relative populations of the energy levels are $1{:}4.6 \times 10^{-2}{:}2.3 \times 10^{-3}{:}1.1 \times 10^{-4}{:}5.3 \times 10^{-5}{:}2.58 \times 10^{-6}$, respectively). All spectra show a narrow peak assigned to the $|-{}^1/_2\rangle-|{}^1/_2\rangle$ transition, superimposed on the broad asymmetric peak of the $|-{}^5/_2\rangle-|-{}^3/_2\rangle$ transition. Although the population of the $M_S = -{}^1/_2$ level is very low, the $|-{}^1/_2\rangle-|{}^1/_2\rangle$ transition is observed due to its small inhomogeneous line width. Unlike the other transitions, the frequency of this transition

(16) Goldfarb, D.; Bernardo, M.; Strohmaier, K. G.; Vaughan, D. E. W.; Thomann, H. *Stud. Surf. Sci. Catal.* **1994**, *84*, 403.
(17) Henning, J. C. M. *Phys. Lett.* **1967**, *24A*, 40.
(18) Gemperle, C.; Schweiger, A. *Chem. Rev.* **1991**, *19*, 1481.
(19) Kurreck, H.; Kirste, B.; Lubitz, W. *Electron Nuclear Double Resonance Spectroscopy of Radicals in Solution*, VCH Publishers, Inc.: New York, 1988; Chapter 3.
(20) Sturgeon, B. E.; Ball, J. A.; Randall, D. W.; Britt, R. D. *J. Phys. Chem.* **1994**, *98*, 1287.
(21) Vardi, R.; Goldfarb, D.; Strohmaier, K. G.; Vaughan, D. E. W.; Bernardo, M.; Thomann, H. In preparation.
(22) Goldfarb, D.; Strohmaier, K. G.; Vaughan, D. E. W.; Bernardo, M.; Thomann, H. Unpublished results.
(23) Vaughan, D. E. W.; Strohmaier, K. G. U.S. Patent 5,185,136, 1993.
(24) Kouwenhoven, H. W.; Stork, W. H. U.S. Patent 4,208,305, 1980.
(25) Disselhorst, J. A. M.; van der Meer, H.; Poluektov, O. G.; Schmidt, J. *J. Magn. Reson. A* **1995**, *115*, 183.
(26) Davies, E. R. *Phys. Lett. A* **1974**, *47A*, 1.
(27) Mims, W. B. *Proc. R. Soc. London* **1965**, *283*, 452.

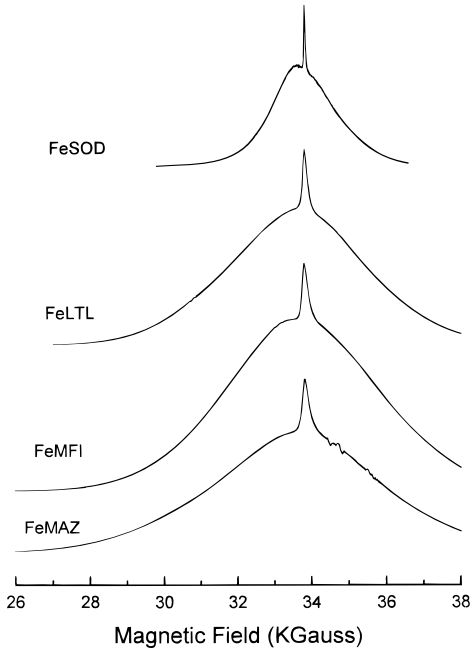

Figure 1. ED-EPR spectra of the zeolites investigated. The upper two spectra were obtained using the two-pulse sequence with $\tau = 0.4$ and 0.5 μs, respectively. The bottom two spectra were recorded using the three-pulse sequence with $\tau = 0.5$ μs and $T = 2$ μs.

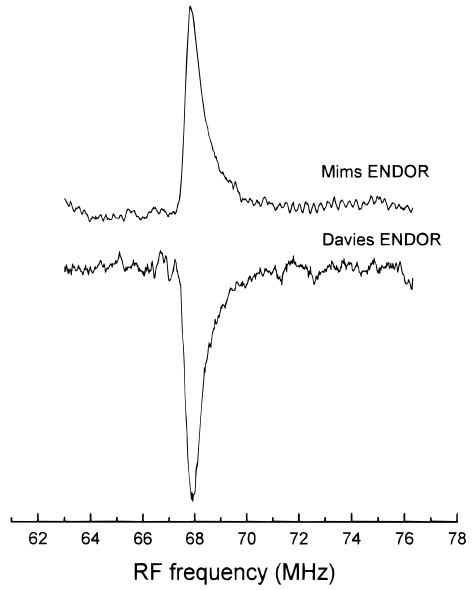

Figure 2. Pulsed ENDOR spectra of ^{57}FeSOD in the region of the ^{57}Fe($M_S = -5/2$) peak: (top) Mims ENDOR ($\tau = 1$ μs, $T = 110$ μs, $t_{RF} = 95$ μs); (bottom) Davies ENDOR ($\tau = 1$ μs, $T = 66$ μs, $t_{RF} = 55$ μs). For both spectra $H_o = 33.856$ kG.

depends on the ZFS only to second order.[28] Since only two out of the five EPR transitions appear, just four ENDOR transitions corresponding to the $M_S = -5/2$, $-3/2$, $-1/2$, and $1/2$ manifolds are expected. The latter two should be observed only at magnetic fields close to $g = 2$. No EPR signals were detected below the range shown in Figure 2, although the X-band spectra of all samples under study, except ^{57}FeSOD, did show signals at low fields ($g \sim 6$ and $g = 4.3$).[15] It is possible that the condition $\nu_e \ll D$, leading to the appearance of the isotropic $g = 4.3$ peak when $E/D = 1/3$,[29] no longer holds at 95 GHz, and the signal suffers from large inhomogeneous broadening which prevents its detection.

The spectrum of ^{57}FeSOD is significantly narrower than those of the other zeolites due to its weaker ZFS interaction. The ZFS parameter, D, was estimated to be $\approx$750 MHz from simulations of the X- and Q- and W-band EPR spectra. The line shape of the ED-EPR spectrum at 95 GHz indicates that D is positive and that $E/D \approx 0.2$. A reasonable agreement between the line shapes of the ED-EPR spectrum and the simulated spectrum was achieved only with a very large line width of $\approx$1200 MHz for the $|-5/2\rangle - |-3/2\rangle$ transition and 90 MHz for the $|-1/2\rangle - |1/2\rangle$ transition. The large line width (1200 MHz) is responsible for the smearing of the powder pattern turning points. One possible explanation for this large line width is the existence of a distribution in the D and E values.[30] Comparison of the width of the powder pattern of ^{57}FeSOD with that of the other zeolites indicates that in ^{57}FeLTL D is 1200−1500 MHz whereas in ^{57}FeMFI and ^{57}FeMAZ it is 1400−1600 MHz. The larger D value in these zeolites is also manifested in the width of the $|-1/2\rangle - |1/2\rangle$ peak which is proportional to D^2/ν_e.[28] The presence of several types of T sites in ^{57}FeLTL, ^{57}FeMAZ, and ^{57}FeMFI, which may exhibit different ZFS parameters, could be another source for broadening.

ENDOR Spectra of ^{57}FeSOD. Figure 2 shows the ^{57}Fe Davies and Mims ENDOR signals corresponding to the $M_S = -5/2$ manifold. The spectra consist of a single peak at 67.8 MHz from which a hyperfine coupling constant of −29.0 MHz is determined using eq 1. This value is in good agreement with the value of −28.8 MHz previously obtained from X-band ENDOR measurements.[21] The frequency of the ^{57}Fe ($M_S = -5/2$) ENDOR signal was found to be practically field independent. This is expected owing to the very low gyromagnetic ratio of ^{57}Fe. A change of 1000 G should introduce a frequency shift of only 0.13 MHz which is within the experimental error.

The amplitude of the inverted echo in the Davies ENDOR experiment is expected to decrease upon the application of a RF pulse at the NMR frequency, thus generating a spectrum with positive peaks, whereas in the Mims ENDOR the positive echo amplitude is expected to decrease by the RF action leading to a spectrum with negative peaks.[18] Note, however, that in the spectra presented in Figure 2 the opposite is observed, the Davies ENDOR signal is negative and the Mims ENDOR signal is positive.

Davies ENDOR spectra in the 34−44 MHz region, recorded at different magnetic fields within the EPR powder pattern, are shown in Figure 3. Spectra recorded with relatively short microwave pulses, which are nonselective with respect to small hyperfine couplings, are depicted in Figure 3A. The spectra exhibit only one field independent signal at 39.0 MHz, assigned to the ^{57}Fe($M_S = -3/2$) transition and yielding $a_{iso} = -29.0$ MHz. This is in good agreement with the value derived from the frequency of the ^{57}Fe($M_S = -5/2$) peak. Note that in contrast to the peak at 67.8 MHz, in these spectra the signal is positive as expected. Davies ENDOR spectra recorded with selective pulses, shown in Figure 3B, exhibit additional peaks, close to the ^{23}Na and ^{27}Al Larmor frequencies. Unlike the ^{57}Fe signal, the frequencies of these peaks do vary with the magnetic field and they are therefore assigned to ^{23}Na and/or ^{27}Al. A close observation of the line shapes in Figure 3B reveals two negative features (marked with arrows) at the low- and high-frequency edges of the spectrum, the frequencies of which also vary with

(28) Abragam, A.; Bleaney, B. *Electron Paramagnetic Resonance of Transition Metal Ions*; Clarendon Press: Oxford, U.K., 1970, pp 156−163.

(29) Castner, T.; Newell, G. W.; Holton, W. C.; Slichter, C. P. *J. Chem. Phys.* **1960**, *32*, 668.

(30) Gaffney, B. J.; Yang, A.-S. *Biophys. J.* **1987**, *51*, 55.

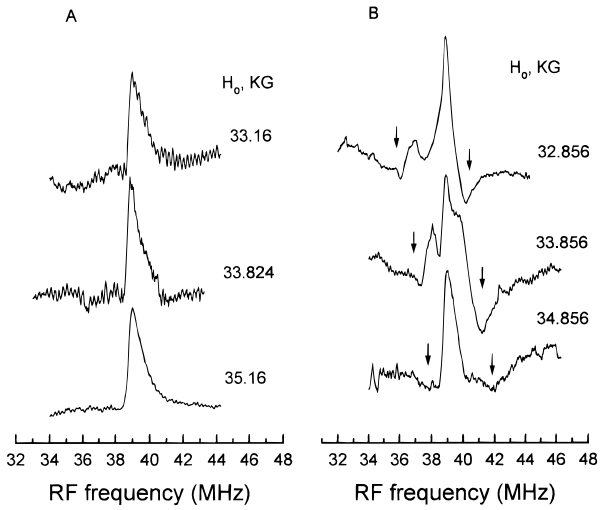

Figure 3. Davies ENDOR spectra of ^{57}FeSOD in the region of the ^{57}Fe($M_S = -3/2$) signal measured at different magnetic fields: (A) nonselective MW pulses, 0.08/0.06/0.08 μs, $T = 53-60$ μs, $t_{RF} = 45-55$ μs; (B) selective MW pulses, 0.4/0.2/0.4 μs, $T = 60$ μs, $t_{RF} = 55$ μs. In both spectra $\tau = 0.5$ μs.

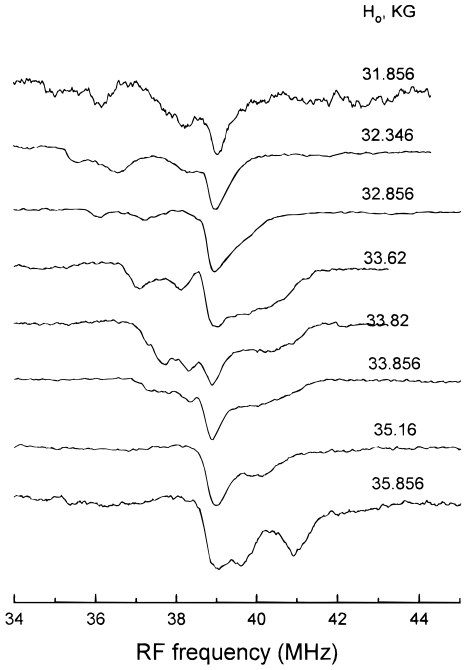

Figure 4. Mims ENDOR spectra of ^{57}FeSOD in the region of the ^{57}Fe($M_S = -3/2$) peak recorded at various magnetic fields within the EPR powder pattern ($\tau = 0.45$ μs, $T = 210$ μs, $t_{RF} = 195$ μs).

the magnetic field. Comparison with the spectra presented in Figure 3A shows that these negative signals are not a consequence of baseline problems. Due to the small couplings, the signals of ^{23}Na and ^{27}Al corresponding to the $M_S = -5/2$ and $-3/2$ manifolds overlap. In analogy to the ^{57}Fe($M_S = -5/2$) signal, the negative signals may be attributed to signals belonging to the $M_S = -5/2$ manifold.

The Mims ENDOR spectra of ^{57}FeSOD in the region of the ^{57}Fe($M_S = -3/2$) line, recorded at different magnetic fields within the EPR powder pattern, are shown in Figure 4. The peaks in these spectra are negative as expected for Mims ENDOR. The spectra consist of four signals, one field independent at 39.0 MHz and three field dependent at 37.7, 38.3 and 40.5 MHz (for $g = 2$). These are the same peaks observed in the Davies ENDOR spectra with selective pulses (Figure 3B). Their field dependence, presented in Figure 5A, is similar to that of the

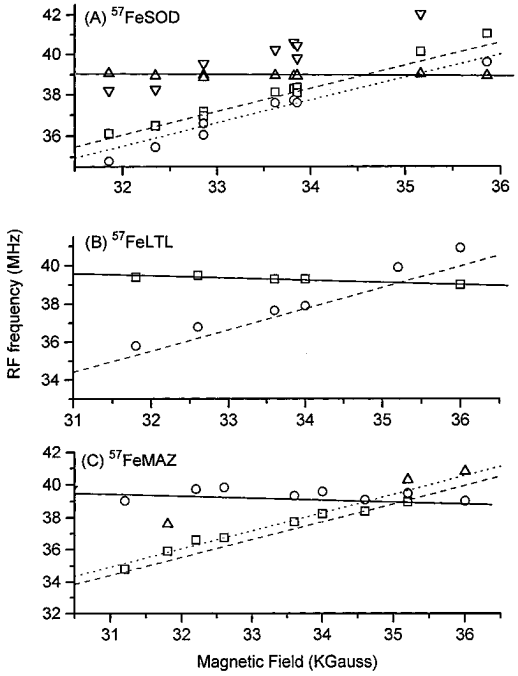

Figure 5. The ENDOR frequencies in the ^{57}Fe($M_S = -3/2$) region as a function of the resonant magnetic field for (A) ^{57}FeSOD, (B) ^{57}FeLTL, and (C) ^{57}FeMAZ. The solid lines represent the ^{57}Fe($M_S = -3/2$) peak, and the dashed and the dotted lines represent the ^{23}Na and ^{27}Al Larmor frequencies, respectively.

Larmor frequencies of ^{27}Al or ^{23}Na. Unfortunately, the close gyromagnetic ratios of ^{27}Al or ^{23}Na prevent the specific assignment of these signals exclusively on the basis of their field dependence.

Mims ENDOR spectra suffer from blind spots when small hyperfine couplings are concerned. The intensity of the ENDOR signals in this case varies with $\sin^2(\Delta\nu\tau)$ where $\Delta\nu = \nu_{ENDOR} - \nu_L$.[18] It is therefore essential to record the spectra at several values of τ to ensure that all ENDOR peaks are indeed detected. Figure 4 shows Mims ENDOR spectra recorded at 33.856 kG at several values of τ. In these spectra the ^{57}Fe($M_S = -3/2$) peak at 39.0 MHz can be used as a reference since for large hyperfine couplings the microwave pulses are selective and the spectra do not suffer from blind spots.[18] These spectra show that the two well-resolved low-frequency peaks observed at $\tau = 0.45$ μ s are actually a consequence of a blind spot in the center of one powder pattern. This is confirmed by comparison with the line shape of the Davies ENDOR spectrum, shown in the top of Figure 6. The relative intensities of the 37.7 and 38.3 MHz signals increase when τ increases from 0.45 to 1.1 μs and the same τ dependence was observed at other magnetic fields. This τ dependence indicates that these signals correspond to small hyperfine couplings, $A < 0.45$ MHz. Unfortunately, we cannot use this τ dependence to assign the signals to ^{27}Al or ^{23}Na because the signals corresponding to the $M_S = -3/2$ and $-5/2$ manifolds cannot be distinguished. These signals can, however, be assigned by comparing the spectra of ^{57}FeSOD with those of ^{57}FeLTL where the exchangeable cations are K^+ rather than Na^+ (see below). This comparison shows that the high-frequency line at $\nu_{ENDOR} = \nu_{Na} + 2.5$ MHz (see Figure 5A) and that appearing at a frequency somewhat lower than ν_{Al} are due to ^{23}Na. The third signal (represented by squares in Figure 5A) is attributed to ^{27}Al.

Although the phases of the peaks in the 30−50 MHz region of the Mims ENDOR spectra are negative as expected, their phase can be inverted by extending the interval T (and t_{RF}) between the second and the last pulse. Changing T from 195

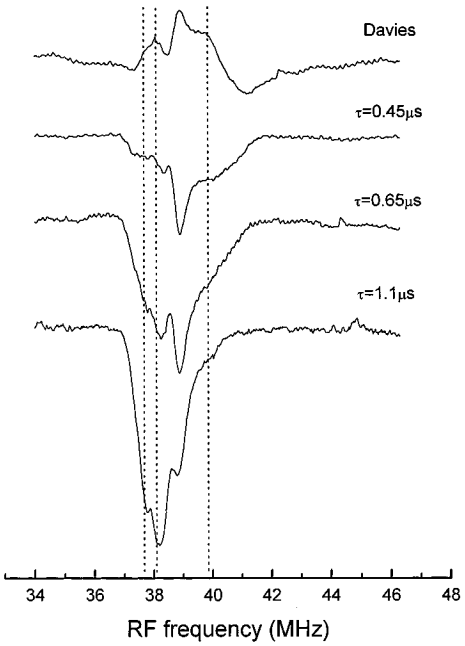

Figure 6. ENDOR spectra of ^{57}FeSOD in the region of the ^{57}Fe($M_S = -3/2$) peak: (top) Davies ENDOR ($\tau = 1$ μs, $T = 66$ μs, $t_{RF} = 55$ μs, microwave pulses 0.4/0.3/0.4 μs); (bottom three spectra) Mims ENDOR spectra as a function of τ ($T = 110$ μs, $t_{RF} = 95$ μs), $H_o = 33.856$ kG.

to 560 μs generated a spectrum with a non-uniform phase across the spectrum, some peaks were positive and some negative. This suggests that the phase of the ENDOR signals is a function of the interval T and/or t_{RF}. We have no explanation for this behavior as yet and believe it is a consequence of some relaxation processes. This phenomenon requires further systematic investigations which are beyond the scope of the present work.

We were not able to observe the ^{57}Fe ENDOR transitions within the $M_S = -1/2, 1/2$ manifolds, expected in the region of 10−20 MHz for $g = 2$, with either the Davies or the Mims ENDOR sequences. We attribute their absence to the low effective RF power at the sample. While the hyperfine enhancement factor for the $M_S = -3/2$ and $-5/2$ manifolds are 10.3 and 16.3, respectively, it is only 4.11 for the $M_S = \pm 1/2$ signals.[19] Therefore, the RF pulse for these ENDOR transitions was far from the ideal value of 180°.

ENDOR Spectra of ^{57}FeLTL. The field dependence of the Mims ENDOR spectra of ^{57}FeLTL in the frequency region 34−44 MHz is shown in Figure 7. The ^{57}Fe($M_S = -3/2$) peak appears at 39.0−39.5 MHz. An increase of 4 kG in the external magnetic field introduced only a slight decrease in the frequency (see Figure 5B) and the hyperfine coupling extracted is −29.4 MHz. The peak of ^{57}Fe($M_S = -5/2$) appears at 68.8 MHz (see Figure 8A), yielding $a_{iso} = -29.2$ MHz, which in a good agreement with the above considering the width of the signal. As in the spectra of ^{57}FeSOD, the phases of the ^{57}Fe($M_S = -5/2$) and ^{57}Fe($M_S = -3/2$) have opposite signs. Another broad signal with a frequency close to ν_{Al} appears in the region of the ^{57}Fe($M_S = -3/2$) peak (Figure 7) and its field dependence is shown in Figure 5B. Its τ dependence is similar to that observed for ^{57}FeSOD, indicating that this ENDOR peak corresponds to a small hyperfine coupling assigned to ^{27}Al since in ^{57}FeLTL the exchangeable cations are K^+ and not Na^+ as in the other zeolites.

Davies ENDOR spectra of ^{57}FeLTL could not be obtained due to the limited RF power at the sample and the relatively short T_1 which affects the intensity of the inverted echo. Although the ENDOR efficiency of the Davies ENDOR

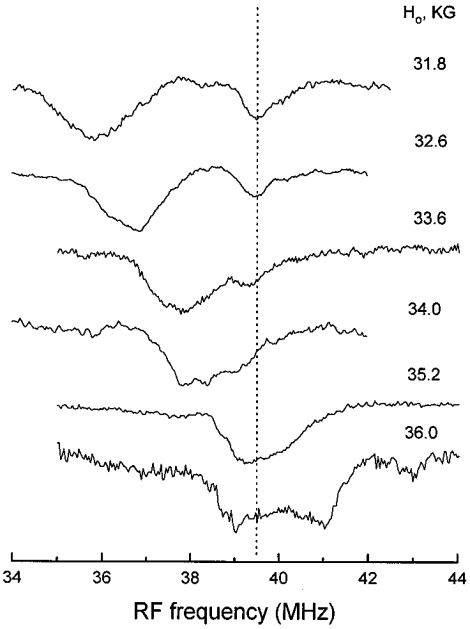

Figure 7. Mims ENDOR spectra of ^{57}FeLTL in the region of the ^{57}Fe($M_S = -3/2$) peak recorded at various magnetic fields within the EPR powder pattern ($\tau = 0.5$ μs, $T = 120$ μs, $t_{RF} = 100$ μs).

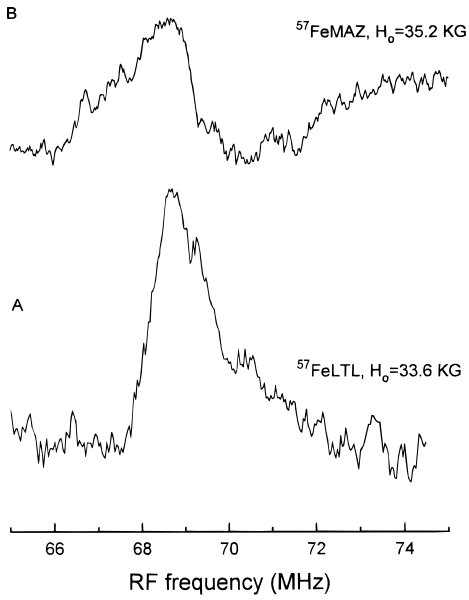

Figure 8. Mims ENDOR spectra in the region of the ^{57}Fe($M_S = -5/2$) peak of ^{57}FeLTL ($H_o = 33.6$ kG) and ^{57}FeMAZ ($H_o = 35.2$ kG), $\tau = 0.5$ μs, $T = 120$ μs, $t_{RF} = 100$ μs.

experiment is larger than that of the Mims ENDOR experiment,[18] we found that it was generally easier to obtain Mims ENDOR spectra because the echo to be sampled was usually more intense. The low RF power required a long RF pulse during which most of the inverted echo in the Davies ENDOR had already relaxed, thus reducing significantly the S/N. In ^{57}FeSOD the spin−lattice relaxation time is significantly longer and the echo remained inverted also with long t_{RF}.

ENDOR Spectra of ^{57}FeMAZ. The ^{57}Fe($M_S = -5/2$) peak of ^{57}FeMAZ appears at 68.7 MHz (see Figure 7b) corresponding to $a_{iso} = -29.4$ MHz and Figure 9 shows the field dependence of the Mims ENDOR spectra in the region of the ^{57}Fe($M_S = -3/2$) signal. Although the S/N is rather poor three signals are observed. As in the other zeolites studied the ^{57}Fe peak overlaps with other signals, but at low fields it is well separated from the ^{27}Al and/or ^{23}Na signals and it yields $a_{iso} = -29.6$ MHz.

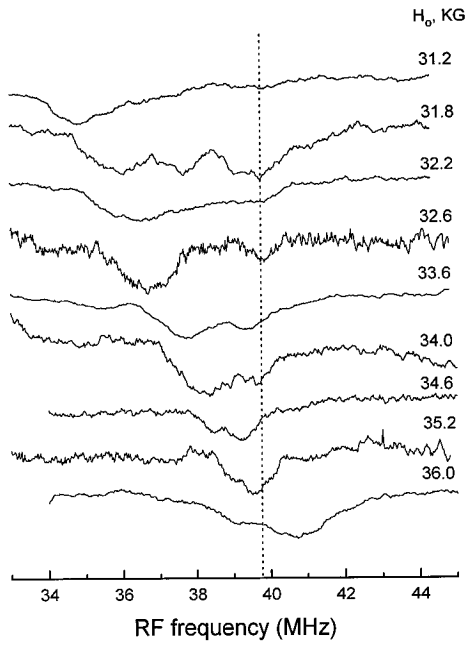

Figure 9. Mims ENDOR spectra of ^{57}FeMAZ in the region of the ^{57}Fe($M_S = -3/2$) peak recorded at various magnetic fields within the EPR powder pattern ($T = 120$ μs, $t_{RF} = 100$ μs, $\tau = 0.5$ μs except for $H_o = 31.2$, 32.2, 33.6 34.6 kG where $\tau = 0.55$ μs).

The dependence of the ENDOR frequencies on the magnetic field is summarized in Figure 5C. The peak with the relatively small coupling, $\nu_{ENDOR} - \nu_{Al} \approx 0.5$ MHz, is assigned to ^{27}Al whereas the signal with a larger coupling, which is well resolved at only one field (31.8 kG), may be due to ^{23}Na.

We had significant difficulties in obtaining ENDOR spectra of ^{57}FeMFI and the S/N was rather poor. One reasonable Mims ENDOR spectrum was however recorded at 34 kG, showing a clear peak at 39.8 MHz. Based on the ENDOR spectra obtained from the other zeolites studied, this signal was assigned to the ^{57}Fe($M_S = -3/2$) and a_{iso} was estimated to be -29.6 MHz.

Discussion

The results presented above demonstrate that the determination of the hyperfine coupling of ^{57}Fe(III) from the ENDOR spectra recorded at 95 GHz is considerably simpler than that at conventional X-band frequencies. At 95 GHz the anisotropy of the ENDOR frequencies introduced through third-order contributions of the ZFS is negligible even for $D \approx 1200$ MHz. Moreover, the second-order hyperfine shifts observed at X-band are eliminated as well. The low-temperature EPR spectrum at 95 GHz is simple and consists of primarily one transition, $|-5/2\rangle - |-3/2\rangle$, compared to the usual five transitions appearing at X-band. Furthermore, the sign of D can be readily determined from the shape of the powder pattern. The simplified EPR spectrum leads to an ENDOR spectrum with only two NMR transitions, the frequencies of which provide directly the magnitude and sign of a_{iso}.

The ^{57}Fe isotropic hyperfine constants of all zeolites investigated were found to be within the range of -29.0 to -29.6 MHz as summarized in Table 2. On the basis of the similar hyperfine constants and the unambiguous assignment of the $g = 2$ signal to Fe(III) in the tetrahedral site for FeSOD,[15] we conclude that in the other zeolites investigated the $g = 2$ signal represents contributions from Fe(III) in the framework sites as well[7,8] and that an isotropic hyperfine coupling in the range of -29.0 to -29.6 MHz is typical for Fe(III) in T sites of zeolites. This range is not surprising since the overall structure and composition of the zeolites studied are different, leading to small variations in the bond angles. These differences are well expressed in the spread of ^{29}Si chemical shifts in zeolites[31] and are expected also to cause some changes in the hyperfine coupling of a paramagnetic T site atom. The different bond angles are probably also responsible for the variations in D. It is interesting that while FeLTL, FeMAZ, and FeMFI have rather similar ZFS parameters, those of FeSOD are significantly smaller. This could be due to the highly symmetric and tight structure of sodalite.

Table 2. ^{57}Fe Isotropic Hyperfine Constants of the Zeolites Investigated as Determined from the ENDOR Frequencies of the $M_S = -3/2$ and $-5/2$ Manifolds

zeolite	a_{iso}, MHz	
	$M_S = -3/2$	$M_S = -5/2$
^{57}FeSOD	29.0	29.0
^{57}FeLTL	29.4	29.2
^{57}FeMAZ	29.4	29.6
^{57}FeMFI	29.6	

Table 3. Isotropic Hyperfine Constant of ^{57}Fe(III) in Various Hosts with Oxygen Coordination Determined by Either ENDOR or Mössbauer Spectroscopy

host	coordination	a_{iso}, MHz	ref
CaO	6, octahedral	29.81	36
MgO	6, octahedral	30.15	36
Al_2O_3	6, octahedral	30.27	37
yttrium iron garnet	6, octahedral	30.25	38
Fe_2O_3	6, octahedral	29.7	39
$RbAl(SO_4)_2 \cdot 12H_2O$	6, trigonal	32.3	40
$RbGa(SO_4)_2 \cdot 12H_2O$	6, trigonal	32.3	40
guanidinium aluminum sulfate hexahydrate	6, trigonal	31.77	41
$Fe(NH_4)(SO_4) \cdot 12H_2O$	6	32.1	42
SnO_2	6, rhombic	30.3, 29.7	43
ferric qhydroxide gels	6	27.24−27.96	44
ZnO	4, tetrahedral	26.9	45
Fe_3O_4	4, tetrahedral	28.15	46
$FePO_4$	4, tetrahedral	28.2	47

The ^{57}Fe(III) isotropic hyperfine constant is sensitive to the degree of covalency and to the geometry of the Fe site. The higher is the degree of covalency, the smaller is a_{iso}.[17] The hyperfine constant of ^{57}Fe(III) in an octahedral environment is in general larger by about 10% than ^{57}Fe(III) in a tetrahedral geometry, although some exceptions have been observed. Table 3 lists a_{iso} values of ^{57}Fe(III) in a number of matrices where it is coordinated to 4 or 6 oxygen atoms in various geometries. The values obtained for Fe(III) in T sites of sodalite, zeolite L, mazzite, and ZSM5 are in general lower than those obtained in octahedral symmetries, but are larger than the value listed for the tetrahedral symmetries. This may be attributed to differences in covalency. The degree of covalency decreases with the increasing electronegativity of the oxygen which in turn is a function of the oxygen environment. A linear relationship between the oxygen electronegativity and the negative ^{29}Si chemical shifts has been established in zeolites.[32] For instance, the presence of Al in the framework is known to reduce the oxygen electronegativity as manifested in the ^{29}Si chemical shift.[31] The chemical shift of a Si surrounded by four O−Al is higher than that surrounded by three O−Al and one O−Si etc. Similarly, the ^{29}Si chemical shift of gallosilicate zeolites is

(31) Engelhardt, G.; Michel, D. *High Resolution Solid State NMR of Silicates and Zeolites*; John Wiley and Sons: New York, 1987; Chapter 4.
(32) Engelhardt, G.; Radeglia, R. *Chem. Phys. Lett.* **1984**, *108*, 271. Radeglia, R.; Engelhardt, G. *Chem. Phys. Lett.* **1985**, *114*, 28.

higher than that of the corresponding aluminosilicate zeolites.[33] Thus, it is not surprising that small differences in a_{iso} were observed considering the different compositions of the zeolites studied. On the basis of the a_{iso} values the degree of covalency of the Fe−O bonds varies in the series investigated according to FeSOD > FeLTL ≈ FeMAZ > FeMFI. This trend happens to correlate with the Al content in the zeolites.

An additional advantage of high-field ENDOR is the observation of resolved ^{27}Al and ^{23}Na signals in ^{57}FeSOD. Unlike the hyperfine interaction of ^{57}Fe, those of ^{27}Al and ^{23}Na are usually anisotropic and the ENDOR frequencies are given to first order by[19]

$$\nu(M_S)_{M_I \leftrightarrow M_{I+1}} = |-\nu_L + M_S(a_{iso} + a_\perp(3\cos^2\theta - 1)| \quad (2)$$

When the point-dipole approximation applies $a_\perp = g\beta g_n\beta_n/hr^3$, and θ is the angle between the vector connecting the paramagnetic center and the coupled nucleus and the external magnetic field, $\vec{H}_o$. In eq 2 the nuclear quadrupole interaction has been neglected. The observation of only two ENDOR transitions is particularly useful in this case since the ENDOR signals corresponding to all M_S manifolds overlap and the reduction in the number of overlapping powder patterns significantly simplifies the spectrum and its analysis.

The larger hyperfine coupling of ^{23}Na in ^{57}FeSOD, as compared to ^{27}Al, shows that the Fe−Na distance is shorter than the Fe−Al distance, as expected for Fe(III) in a T site. In this site the Fe(III) is surrounded by a tetrahedral arrangement of four Na^+ ions, each situated on the symmetry axis of the 6-member ring, with a Fe−Na distance of 3.35 Å,[34] corresponding to $a_\perp = 0.56$ MHz. The Fe(III) most probably substitutes for Al and according to the Loewenstein rule it should be surrounded by four Si atoms in its second shell and Al will appear only in the fourth shell with a minimal distance of ≈4.5 or ≈5.4 Å, depending on whether the Al is across a four ring or a six ring.[34] These distances correspond to very small $a_\perp$ values, 0.22 and 0.12 MHz, respectively. The Fe framework site is negatively charged and its proximity to positive Na^+ ions is thus of no surprise. However, if the Fe(III) ions were in extra-framework locations, due to their positive charge they would have been situated close to negative framework Al sites rather than to positive Na ions. The small ^{27}Al hyperfine couplings found in the other zeolites investigated support the assignment of at least part of the Fe(III) with the $g = 2$ signal to T sites.

Unfortunately, the line shapes of the ^{23}Na signals are not well resolved and distinct powder patterns cannot be extracted. In Mims ENDOR spectra blind spots corrupt the line shape and in Davies ENDOR signals with small couplings may have reduced intensities. Additional complications arise from the change of the phase of the signal due to the very long RF pulse. The latter observation, however, can be used to obtain the isotropic and anisotropic hyperfine components of the ^{23}Na ions. Assuming that the two negative signals at the edges of the Davies ENDOR correspond to the turning points ($\theta = 0°$, 90° in eq 2) of the inverted powder pattern of the $M_S = -5/2$ manifold, a powder pattern with a total width of 4 MHz is obtained, as indicated by the arrows in Figure 3B. From this width and using eq 2 a value of 0.53 MHz is obtained for $a_\perp$. Once the parallel ($\theta = 0°$) and perpendicular ($\theta = 90°$) turning points of the powder pattern are assigned it is also possible to calculate a_{iso} using eq 2. Although the low-frequency signal seems less intense, we cannot attribute it to the parallel singularity due to the reasons mentioned above. We thus considered both options in our calculations. Only by taking the low-frequency signal as the perpendicular edge was the same a_{iso} value (0.15 MHz) determined from the two negative signals. The validity of this assignment was further evaluated by calculating the parallel and perpendicular singularities of the $M_S = -3/2$ powder pattern using the above a_{iso} and $a_\perp$ and eq 2, yielding perpendicular and parallel singularities at 39.9 and 37.5 MHz, respectively (at $H_o = 33.856$ kG). This is in reasonable agreement with spectral features observed in Figure 3B and with the peak assignment of ^{57}FeSOD based on the comparison with ^{57}FeLTL. The ^{23}Na anisotropic hyperfine component, $a_\perp$, of 0.53 MHz corresponds to a distance of 3.4 Å which is in excellent agreement with the distance 3.35 Å obtained from X-ray measurements for Si(Al)−Na in sodalites.[34] In the above analysis the ^{23}Na quadrupole interactions have been neglected. This assumption is justified since the quadrupole interaction is relatively small as indicated by the readily observed ^{23}Na NMR spectrum of sodalite.[35]

Conclusions

The hyperfine interaction of ^{57}Fe(III) in T sites of sodalite, zeolite L, mazzite, and ZSM5 was found to be isotropic with a_{iso} in the range of −29.0 to −29.6 MHz. In the case of FeSOD superhyperfine couplings of ^{23}Na were detected as well and the corresponding isotropic (0.15 MHz) and anisotropic components (0.53 MHz) were determined. These values provide additional evidence for the location of the Fe(III) in framework T sites. This work demonstrates the great potential of high-field pulsed ENDOR for high-spin systems where complicating second- and third-order broadening effects are eliminated and the number of transitions observed is reduced.

Acknowledgment. We thank Rotem Vardi for performing the simulations of the EPR spectra of ^{57}FeSOD.

JA953903E

(33) Engelhardt, G.; Michel, D. *High Resolution Solid State NMR of Silicates and Zeolites*; John Wiley and Sons: New York, 1987; Chapter 4, p 254.
(34) Löns, V. J.; Schultz, H. *Acta Crystallogr.*, **1967**, *23*, 434.
(35) Engelhardt, G.; Koller, H.; Seiger, P.; Repmeier, W.; Samoson, A. *Solid Stat. Nucl. Magn. Reson.* **1992**, *1*, 127. Engelhardt, G.; Buhl, J.-Ch.; Felsche, J.; Foerster, H. *Chem. Phys. Lett.* **1088**, *153*, 332.
(36) Locher, P. R.; Geschwind, S. *Phys. Rev.* **1965**, *139*, A991.
(37) Wertheim, G. K.; Reimeika, J. P. *Phys. Lett.* **1964**, *10*, 14.
(38) Boutron, F.; Robert, *C. C. R. Acad. Sci.* **1961**, *253*, 433.
(39) Nakamura, T.; Shimizu, S. *Bull. Inst. Chem. Res., Kyoto Univ.* **1964**, *42*, 299.
(40) Brisson, J. R.; Manoogian, A. *Phys. Rev. B* **1978**, *18*, 4576.
(41) Misra, S.; Van-Ormondt, D. *Phys. Rev. B* **1984**, *30*, 6327.
(42) Edwards, P. R.; Johnson, C. E. *J. Chem. Phys.* **1968**, *49*, 211.
(43) Rhein, W. *Z. Naturforsch.* **1972**, *27*, 741.
(44) Okamoto, S.; Sekizawa, H. *J. Phys.* **1979**, *40*, C2−137.
(45) Walsh, W. M.; Rupp, u. L. W. *Phys. Rev.* **1962**, *126*, 952.
(46) Ranerjee, S. K.; O'Reilly, W.; Johnson, C. E. *J. Appl. Phys.* **1967**, *38*, 1289.
(47) Bruckner, W.; Fuchs, W.; Ritter, G. *Phys. Lett.* **1967**, *26A*, 32.